The Astrophysical Journal Letters, 933:L18 (6pp), 2022 July 1 https://doi.org/10.3847/2041-8213/ac79af

Multiplicity Statistics of Stars in the Sagittarius Dwarf Spheroidal Galaxy: Comparison to the Milky Way

Victoria Bonidie[1,2], Travis Court[1,2], Christine Mazzola Daher[1,2], Catherine E. Fielder[1,2], Carles Badenes[1,2], Jeffrey Newman[1,2], Maxwell Moe[3], Kaitlin M. Kratter[3], Matthew G. Walker[4], Steven R. Majewski[5], Christian R. Hayes[6], Sten Hasselquist[7], Keivan Stassun[8], Marina Kounkel[8], Don Dixon[8], Guy S. Stringfellow[9], Joleen K. Carlberg[10], Borja Anguiano[11], Nathan De Lee[12], and Nicholas W. Troup[13]
[1] Department of Physics and Astronomy, University of Pittsburgh, 3941 O'Hara Street, Pittsburgh, PA 15260, USA
[2] Pittsburgh Particle Physics, Astrophysics, and Cosmology Center (PITT PACC), University of Pittsburgh, Pittsburgh, PA 15260, USA
[3] Steward Observatory, University of Arizona, 933 N. Cherry Avenue, Tucson, AZ 85721, USA
[4] McWilliams Center for Cosmology, Department of Physics, Carnegie Mellon University, 5000 Forbes Avenue, Pittsburgh, PA 15213, USA
[5] Department of Astronomy, University of Virginia, P.O. Box 400325, Charlottesville, VA 22904-4325 USA
[6] NRC Herzberg Astronomy and Astrophysics, 5071 West Saanich Road, Victoria, BC V9E 2E7, Canada
[7] New Mexico State University, Las Cruces, NM 88003, USA
[8] Department of Physics and Astronomy, Vanderbilt University, Nashville, TN 37235, USA
[9] Center for Astrophysics and Space Astronomy, Department of Astrophysical and Planetary Sciences, University of Colorado, 389 UCB, Boulder, CO 80309-0389, USA
[10] Space Telescope Science Institute, 3700 San Martin Drive, Baltimore, MD 21218, USA
[11] Department of Astronomy, University of Virginia, Charlottesville, VA 22904, USA
[12] Department of Physics, Geology, and Engineering Tech, Northern Kentucky University, Highland Heights, KY 41099, USA
[13] Department of Physics, Salisbury University, Salisbury, MD 21801, USA
Received 2022 April 15; revised 2022 June 2; accepted 2022 June 14; published 2022 June 30

Abstract

We use time-resolved spectra from the Apache Point Observatory Galactic Evolution Experiment (APOGEE) to examine the distribution of radial velocity (RV) variations in 249 stars identified as members of the Sagittarius (Sgr) dwarf spheroidal (dSph) galaxy by Hayes et al. We select Milky Way (MW) stars that have stellar parameters ($\log(g)$, $T_{\rm eff}$, and [Fe/H]) similar to those of the Sagittarius members by means of a k-d tree of dimension 3. We find that the shape of the distribution of RV shifts in Sgr dSph stars is similar to that measured in their MW analogs, but the total fraction of RV variable stars in the Sgr dSph is larger by a factor of $\sim$2. After ruling out other explanations for this difference, we conclude that the fraction of close binaries in the Sgr dSph is intrinsically higher than in the MW. We discuss the implications of this result for the physical processes leading to the formation of close binaries in dwarf spheroidal and spiral galaxies.

Unified Astronomy Thesaurus concepts: Sagittarius dwarf spheroidal galaxy (1423); Spectroscopic binary stars (1557); K giant stars (877)

1. Introduction

The Sagittarius (Sgr) dwarf spheroidal (dSph) galaxy (Ibata et al. 1994) is one of the closest and largest satellites of the Milky Way (MW), and presents a unique opportunity to explore the stellar content of a galaxy outside of our own in detail. Recent studies have used a combination of 3D positions and kinematics to identify nearby stars as members of the Sgr dSph (Hasselquist et al. 2017; Hayes et al. 2020). Many of these objects now have multiepoch, high signal-to-noise, high-resolution spectroscopy from the Apache Point Observatory Galactic Evolution Experiment (APOGEE; Majewski et al. 2017; Wilson et al. 2019), one of the core surveys of the Sloan Digital Sky Survey IV (SDSS-IV; Gunn et al. 2006; Blanton et al. 2017). Most of the Sgr dSph members observed by APOGEE also have high-quality parallaxes from Gaia (Gaia Collaboration et al. 2018; Sanders & Das 2018), and are thus among the best-studied stars known to have formed outside our Galaxy.

Here we leverage the opportunity offered by these observations to examine the stellar multiplicity statistics in the Sgr dSph. The multiepoch feature of the APOGEE spectra allows us to measure high-precision radial velocities (RVs; Nidever et al. 2015) from Doppler shifts in the visit spectra, and define a maximum RV shift, $\Delta {\rm RV}_{\rm max} = |{\rm RV}_{\rm max} - {\rm RV}_{\rm min}|$, for each star. This figure of merit is a reliable indicator for the presence of short-period binary companions, and it can be used to put constraints on multiplicity statistics (see Badenes & Maoz 2012; Maoz et al. 2012 for discussions). Previous studies have shown that RV variability is a strong function of stellar parameters (Moe & Di Stefano 2017). For the cool ($T_{\rm eff} \lesssim 6500$ K) stars targeted by APOGEE, the parameters with the strongest correlation to RV variability are $\log(g)$ (due to the attrition of the shortest-period companions as stars ascend the red giant branch; Badenes et al. 2018) and chemical composition (due to the strong anticorrelation between the close binary fraction, metallicity, and α abundances; Badenes et al. 2018; Moe et al. 2019; Mazzola et al. 2020), with $T_{\rm eff}$ playing a more secondary role (Mazzola et al. 2020; Price-Whelan et al. 2020).

A complete characterization of the relationship between stellar parameters, $\Delta {\rm RV}_{\rm max}$ distributions, and multiplicity statistics requires large sample sizes for a robust multivariate analysis (e.g., Mazzola et al. 2020), but this approach is not

feasible for the small number of stars identified as members of the Sgr dSph. Here we propose an alternative method to constrain multiplicity statistics using relatively small samples. This method takes advantage of the large number of MW stars observed with APOGEE to define a control sample of stellar analogs matched on physically motivated parameters. A statistical comparison between the RV shifts in the sample under study and the MW analogs can reveal differences in the underlying multiplicity statistics, which, if present, should be caused by parameters that have not been controlled for in the generation of the analog sample.

The characterization of the fundamental statistics of stellar multiplicity (the distribution of periods, eccentricities, and mass ratios) remains an important problem in stellar astrophysics (Moe & Di Stefano 2017). It is a particularly relevant issue for dSph galaxies, given that inferences on the dark matter content of these objects can be easily biased by the presence of a few short-period binaries (McConnachie & Côté 2010; Koposov et al. 2011; Buttry et al. 2021). Multiepoch RV data sets have been used in the past to put constraints on the multiplicity statistics of dSph galaxies (e.g., Martinez et al. 2011; Simon et al. 2011), but our goal is to make a direct comparison of the RV variability statistics between two samples of similar stars in the Sgr dSph and the MW. This comparison will help us elucidate whether the physical mechanisms responsible for the formation of close binaries operate differently in dark-matter-dominated dwarf galaxies and star-forming spirals (e.g., Minor et al. 2019; Wyse et al. 2020).

This Letter is organized as follows. In Section 2.1, we describe the sample of Sgr dSph members from Hayes et al. (2020) and the quality cuts we apply to measure RV variability. In Section 2.2, we discuss the method used to select the MW analog sample, which we compare to the Sgr dSph sample in Section 3, along with a brief discussion of the physical interpretation of this comparison.

2. Methods

2.1. Sagittarius Sample Selection

The sample of Sgr dSph members published by Hayes et al. (2020) relies on APOGEE data release 16 (Ahumada et al. 2020; Jönsson et al. 2020), and adds 518 new stars to the 325 previously identified in Hasselquist et al. (2017), for a total of 876 members. These stars were selected using a combination of chemical tagging and 3D positions and velocities relative to the Sgr orbital plane, with additional cuts imposed to minimize contamination from MW halo stars. The identified Sgr members sample both the core of the dSph galaxy and the trailing and leading arms of the stream.

In order to make robust measurements of RV variability for these Sgr dSph members, we introduced the quality cuts described in Mazzola et al. (2020), which remove stars targeted as telluric calibrators, star cluster members, and commissioning stars, and require acceptable ($\neq$9999) values for $T_{\rm eff}$, $\log(g)$, and [Fe/H] in the APOGEE Stellar Parameter and Chemical Abundances Pipeline (ASPCAP; García Pérez et al. 2016; Jönsson et al. 2020). For the RV measurements, we used the VISITS_PK indices (Holtzman et al. 2015; Nidever et al. 2015) to select the individual visits that were included in each combined APOGEE spectrum, and we required that each star have two or more visit spectra with a signal-to-noise ratio (S/N) $\geqslant$ 40. A total of 249 Sgr dSph members survived these cuts, 48 in the extended stellar stream and 201 in the core (Hasselquist et al. 2017).

2.2. Analog Sample Selection

To select stellar analogs to the Sgr dSph members, we begin by imposing the combined quality cuts from Hayes et al. (2020) and Mazzola et al. (2020) on all the stars in APOGEE DR16. This results in an initial sample of 188,104 MW stars for which we can extract stellar parameters and RV measurements of at least the same quality as the Sgr dSph members. Since most MW stars are closer and brighter than the Sgr dSph members, their spectra can have much larger S/Ns. To ensure that the presence of MW stars with very high S/N spectra does not introduce unwanted biases in our measurements, we require that the S/N of the stellar analogs be in the same range as the Sgr dSph members ($53 < {\rm S/N} < 283$), leaving us with a sample of 139,983 MW stars from which to draw our analogs. We note that this additional restriction on the MW analogs does not affect the results described below.

Our method to select stellar analogs to the Sgr dSph members from the main APOGEE DR16 sample is based on methods described in Licquia et al. (2015) and Fielder et al. (2021). The goal is to define a large enough sample of MW stars whose parameters have statistical distributions that are similar to those of the Sgr dSph members. Because RV variability in APOGEE targets is driven mainly by location in the Hertzsprung–Russell diagram and chemical composition (Mazzola et al. 2020), we choose $\log(g)$, $T_{\rm eff}$, and [Fe/H] as the parameters for analog selection. We note that the relationship between stellar multiplicity and chemical composition is complex, and that α abundances in particular can have a strong impact on multiplicity statistics at fixed [Fe/H] (see Mazzola et al. 2020 for a discussion). However, we find that the introduction of additional selection parameters results in nonviable analog sample sizes. We will revisit the impact of α abundances on our measurements in Section 3.

To optimize the search for analogs in multidimensional space, we use a k-d tree, which is a binary tree with points in k-dimensional space (Bentley 1975). Given a star A in the Sgr dSph member sample, we standardize the values for all the stars in our main MW sample, subtracting from each parameter the value measured in star A and dividing by its standard deviation (i.e., the measurement uncertainty). This ensures that all data are on the same scale when put into the tree. We then use the `spatial.cKdDTree` routine from Virtanen et al. (2020) to construct a k-d tree from this scaled data, which we query to find the closest N neighbors to star A in the three-dimensional space of selection parameters. We performed a series of a Kolmogorov–Smirnov (K-S) tests on the distributions of $T_{\rm eff}$, $\log(g)$, and [Fe/H] between the analog and Sgr samples as a function of neighbor number, and we found that $N = 20$ offers a good compromise between sample size and similarity of the resulting distributions. To further restrict the distance of the selected neighbors, we require the analog candidate's parameters to fall within one standard deviation of the mean parameters of star A.

After the 20 nearest neighbors to star A are selected, a single analog must be chosen among them. To do this, we assign weights to each neighbor based on their distance in parameter

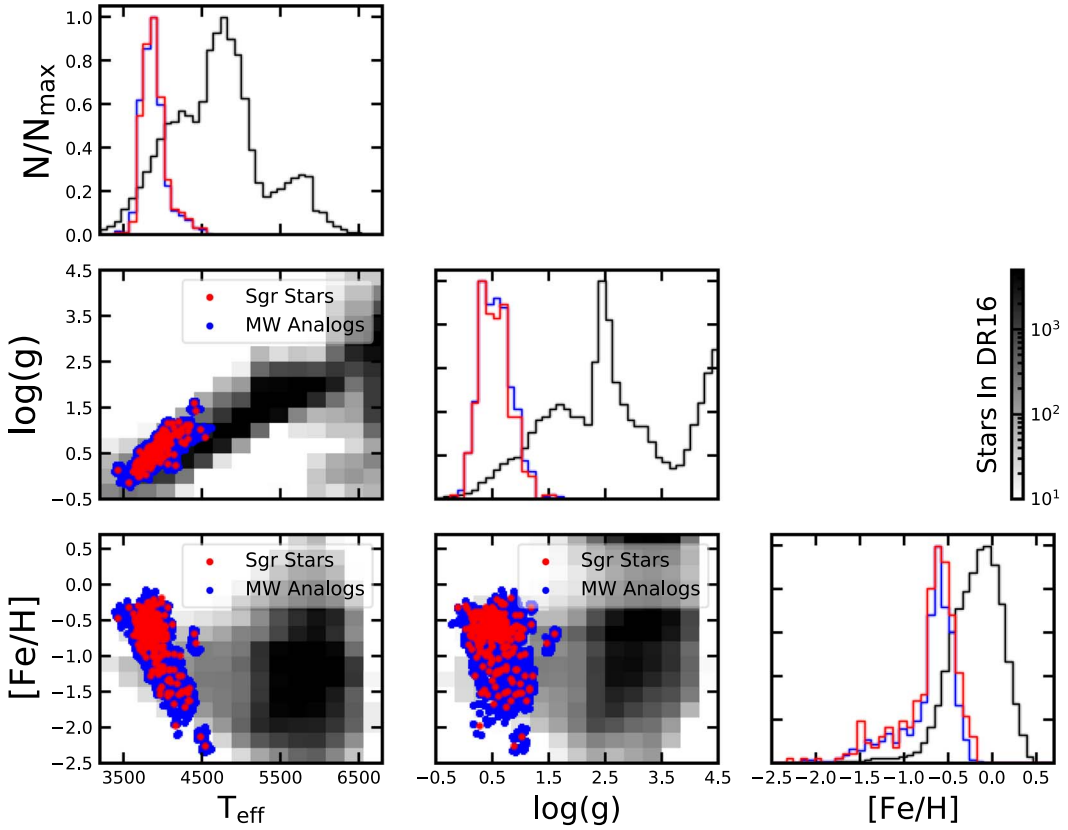

Figure 1. Triangle plot of the pairwise distributions of $T_{\rm eff}$, $\log(g)$, and [Fe/H] for the full APOGEE DR16 sample (shaded two-dimensional histograms), along with the Sgr dSph members (red points) and their MW analogs (blue points). The one-dimensional histograms along the diagonal show the normalized distributions for each parameter individually.

space from the query point. Our weights (w) are equal to

$$w = \frac{e^{-d^2/2}}{\sum(e^{-d^2/2})}, \quad (1)$$

where d is the Euclidean distance in parameter space to the neighbor (e.g., $d(\boldsymbol{x}, \boldsymbol{y}) = \sqrt{\sum_{i=1}^{n}(x_i - y_i)^2}$ for two n-dimensional vectors). The analog to star A is then selected from a random draw among these neighbors, using these weights. The selection then proceeds as outlined in Licquia et al. (2015). Using this procedure, we obtain 100 MW analogs for each star in the Sgr dSph member sample, resulting in a total sample of 24,900 analog stars, of which 1679 are unique. Repetition of analogs for each star is necessary to ensure that the probability distributions of the selection parameters in the analog sample closely match those in the Sgr dSph sample (Licquia et al. 2015). The Galactic analog search code is publicly available at the Milky Way analog GitHub page.[14] The stellar version of the code, used in the work presented here, is available upon request.

Figure 1 shows a comparison between the stars in the Sgr dSph member sample and our MW analog sample in the three-dimensional space of selection parameters, along with the main APOGEE DR16 sample, which is included for illustrative purposes. As expected, the distribution of values in the MW analog sample closely matches that of the Sgr dSph sample on all three selection parameters ($T_{\rm eff}$, log(g), and [Fe/H]). A K-S test on the selection parameter distributions for the two samples yields p-values of 0.496 for $T_{\rm eff}$, 0.756 for log(g), and 0.072 for [Fe/H]. Since all p-values are above 0.05, we conclude that the samples are well matched. Our MW analog sample spans the entire range of R.A. and decl. in DR16, indicating that we are not preferentially selecting stars from any specific regions or substructures in the Milky Way. We also confirm that the distributions of the number of visits are similar between both samples.

3. Results and Discussion: Stellar Multiplicity in the Sagittarius Dwarf Spheroidal

We now have two samples of metal-poor K-type giants that are closely matched on three selection parameters ($\log(g)$, $T_{\rm eff}$, and [Fe/H]), one composed of Sgr dSph members and one of MW stars. We can compare the multiplicity statistics of these two samples through the distributions of ΔRV_{max} values, which are shown in Figure 2. In this plot, the red squares represent the histogram of ΔRV_{max} values in the Sgr dSph sample, while the shaded region represents the statistical range (50th rank in black, 16th–84th ranks in dark blue, and 2nd–98th ranks in light blue) of the ΔRV_{max} distributions found in the 100 MW analog subsamples with $N = N_{\rm Sgr} = 249$ that can be constructed by random draw from the main MW analog sample.

The distribution of ΔRV_{max} values in a sample of stars with multiple RV measurements of good quality is characterized by a "core" of systems with low ΔRV_{max} , composed of wide binaries and single stars, and a distinct "tail" of systems at high

[14] https://github.com/cfielder/Milky-Way-Analogs. This code is provided under a CC BY-SA 4.0 license.

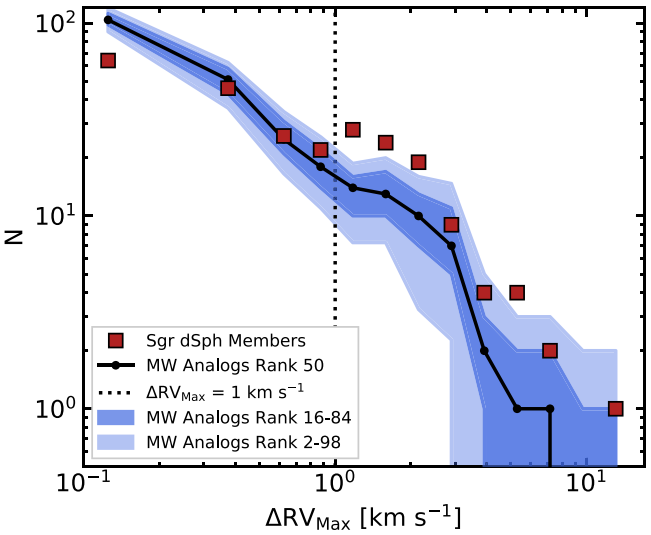

Figure 2. Histogram of ΔRV_{max} values measured in the Sgr dSph members (red squares), together with the range of values found in the MW analogs (solid black line for the 50th rank, dark and light shaded regions for the 16th–84th and 2nd–98th ranks, respectively). For illustrative purposes, we highlight a ΔRV_{max} value of 1 km s^{-1} with a vertical dotted line.

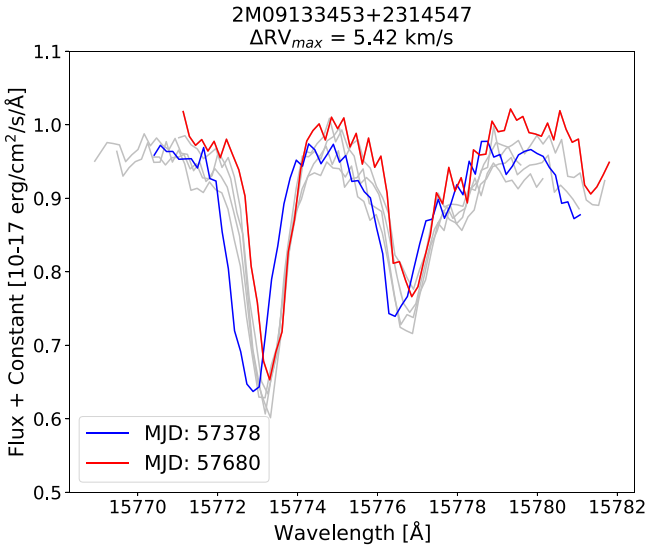

Figure 3. The visit spectra for the Sgr dSph member, 2M09133453+2314547, shown around the Fe II line at 15,773.5860 Å and the Fe I line at 15,776.733 Å (Kramida et al. 2021). The ΔRV_{max} for this star is 5.42 km s^{-1}, corresponding to the difference between the visit spectra highlighted in red (MJD 57680) and blue (MJD 57378).

ΔRV_{max} that is dominated by short-period binaries. The shape and extent of the "core" of the distribution, and the location of the "core"/"tail" transition, are mainly driven by the distribution of RV errors, which can be difficult to characterize (see Maoz et al. 2012 and Mazzola et al. 2020 for discussions). Badenes et al. (2018) found that the dwarfs and most of the giants observed by APOGEE have "core"/"tail" transitions around 1 or 2 km s^{-1}, but metal-poor giants close to the tip of the RGB can have broader cores (see their Figure 9 and related discussion in their Section 3.3). However, as long as both the Sgr dSph member sample and the MW analog sample contain enough bona fide short-period binaries at high values of ΔRV_{max}, it is not necessary to specify a threshold value to compare the distributions. To ensure that this is the case, we visually inspected the visit spectra for each Sgr dSph member with $\Delta RV_{max} > 3$ km s^{-1}, and confirmed they all have clear Doppler shifts; we show an example in Figure 3 with $\Delta RV_{max} = 5.42$ km s^{-1}. Unfortunately, none of our Sgr stars appear in the *Gold* sample from Price-Whelan et al. (2020), so we do not have any estimates for their orbital parameters from The Joker (Price-Whelan et al. 2017). This is unsurprising, given that the vast majority of the stars in our Sgr sample have very sparsely sampled RV curves (76% have only two or three RVs). Regardless, the presence of bona fide short-period binaries like the system shown in Figure 3 confirms that the ΔRV_{max} distributions can be used to constrain the multiplicity statistics of the underlying stellar populations.

We directly compare the ΔRV_{max} distributions of the Sgr dSph stars and their MW analogs by means of an Anderson–Darling (A-D) test. This statistic gives more weight to the "tails" of the distributions, i.e., our region of interest for binaries, more so than the commonly used K-S test, which instead is most sensitive to differences in the core of a distribution. The A-D test yields a p-value below 0.001, which is the floor of the test. This allows us to reject the null hypothesis that the underlying distributions are identical. Indeed, even though the high ΔRV_{max} "tails" shown in Figure 2 have similar shapes, the Sgr dSph stars clearly have a larger RV variability fraction, with star counts always above the median and often beyond the 98th rank of the MW analogs. We further illustrate this point in Figure 4, which shows the total number of stars with ΔRV_{max} above a certain threshold, as a function of the threshold value. The number of RV variable stars in the Sgr dSph sample is consistently above the 98th rank of the numbers seen in the MW analog samples. Crucially, this does not depend on the value of the threshold we choose for RV variability (i.e., the location of the vertical dotted line in Figure 2), well into the regime where we have visually inspected every star to confirm that the RV shifts are real. This means that an extended tail of RV errors cannot be responsible for the higher fraction of RV variables seen in the Sgr dSph sample. We also note that the ratio of Sgr dSph to MW analog RV variables does not change when the samples are split into high and low [Fe/H] along the median.

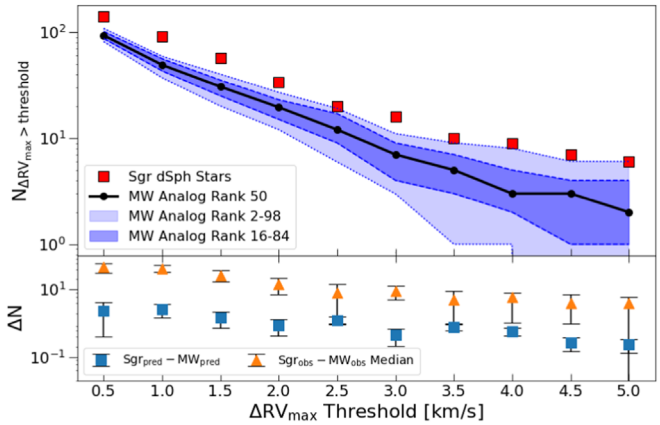

Figure 4. Upper panel: number of Sgr dSph stars with ΔRV_{max} above the given threshold (red squares), together with the 50th rank (black line), 16th–84th ranks (dark blue region), and 2nd–98th ranks (light blue region) of values seen in the MW analog samples. Lower panel: difference between the number of RV variable stars measured in the Sgr and MW analog samples (orange triangles), alongside our estimate for the difference that would arise from the offset of [α/H] values between the samples (blue squares).

To explain the larger fraction of RV variables among Sgr dSph stars without invoking different multiplicity statistics, the RV variability would have to be linked to a parameter or parameters that were not controlled for in the analog selection process. Among the parameters that were left out of the k-d tree, α abundances have the strongest correlation with RV variability in APOGEE targets (Mazzola et al. 2020). Indeed, the values of [α/H] in the Sgr dSph stars are ∼0.13 dex lower than those of their MW analogs, which is consistent with the known chemistry of the Sgr dSph galaxy (Sbordone et al. 2007), and should lead to higher RV variability (Mazzola et al. 2020). To quantify the impact that this offset in [α/H] might have on RV variability, we used a sample of 31,176 giants in APOGEE ($\log(g) < 1.5$, $T_{\rm eff} < 4500$ K) to estimate the RV variability fractions of the Sgr and MW analog samples based on their [Fe/H] and [α/H] values. For each Sgr and MW analog star, we identified the bin in [Fe/H] –[α/H] space that it corresponds to in the sample of giants, and assigned it the RV variability fraction and associated uncertainty of that bin. These weighted averages can be used to estimate the increase in RV variability that we would see just from the fact that the [α/H] values of stars in the Sgr sample are lower than those in their MW analogs. This increase is shown in the lower panel of Figure 4, and is in all cases smaller than the actual difference in RV variability measured between the Sgr and MW analog samples.

We conclude that the increased fraction of RV variables seen among Sgr dSph stars is too large to be explained by the systematic difference in [α/H] between those stars and their MW analogs. Our analysis suggests that the close binary fraction in the Sgr dSph sample is in fact higher than in the MW analogs, by a factor ∼2, which is relatively insensitive to the choice of ΔRV_{max} threshold. This result is consistent with the predictions made by Marks & Kroupa (2011), who claim that the environments of ellipticals, spirals, and dwarf galaxies should lead to different field binary fractions for main-sequence stars and predicts that dwarf galaxies should have a higher binary fraction among main-sequence stars than the MW. The physical reason for this higher fraction of close binaries is unclear at this stage. Wyse et al. (2020) found an enhanced occurrence rate of blue stragglers in metal-poor dSph galaxies, including Sgr, which they attributed to the metallicity dependence of the close binary fraction and the outcome of processes such as dynamical friction and mass segregation. Mass segregation through two-body interactions is known to operate in relaxed stellar systems, driving the heavier binaries to the bottom of the potential well. However, given the properties of the Sgr dSph (Gibbons et al. 2017), it is unlikely that the system was relaxed before being accreted by the MW (Binney & Tremaine 2008). In any case, the number of stars from the Sgr dSph stream in our sample (48) is too small to firmly establish whether the fraction of RV variables among them is higher or lower than in the core of the Sgr dSph, as would be predicted by this scenario. In our sample, the fraction of stars with $\Delta RV_{max} > 1$ km s^{-1} in the stream is 0.40 ± 0.07 and that of the core is 0.36 ± 0.03. The error bars on the RV variability fractions are too large, and their behavior as a function of ΔRV_{max} is too noisy, to confirm or rule out mass segregation as the origin of the higher RV variability in the Sgr dSph. Finally, we note that the methods we have described in this Letter can be applied to other systems in the Local Group with similar data from APOGEE and other samples, like the Magellanic Clouds or the Gaia–Enceladus sausage (Sanders et al. 2021). In this way, it would be possible to explore systematic variations in stellar multiplicity statistics across different dynamical environments using relatively small samples of sparsely sampled RV curves.

V.B. acknowledges support from a Whittington Fellowship awarded by the Dietrich School of Arts and Sciences at the University of Pittsburgh. C.M.D. and C.B. acknowledge support from the National Science Foundation grant AST-1909022. C.E.F. acknowledges support from NASA Astrophysics Data Analysis Program grant number 80NSSC19K0588.

This work made use of Python, along with many community-developed or maintained software packages, including IPython (Perez & Granger 2007), Jupyter (jupyter.org), Matplotlib (Hunter 2007), NumPy (van der Walt et al. 2011), Pandas (McKinney 2010), scikit-learn (Pedregosa et al. 2011), and SciPy (Virtanen et al. 2020). This research made use of NASA's Astrophysics Data System for bibliographic information.

ORCID iDs

Victoria Bonidie https://orcid.org/0000-0001-5330-7709
Travis Court https://orcid.org/0000-0003-3837-7201
Christine Mazzola Daher https://orcid.org/0000-0003-2116-2159
Catherine E. Fielder https://orcid.org/0000-0001-8245-779X
Carles Badenes https://orcid.org/0000-0003-3494-343X
Jeffrey Newman https://orcid.org/0000-0001-8684-2222
Maxwell Moe https://orcid.org/0000-0002-0870-6388
Kaitlin M. Kratter https://orcid.org/0000-0001-5253-1338
Matthew G. Walker https://orcid.org/0000-0003-2496-1925
Steven R. Majewski https://orcid.org/0000-0003-2025-3147
Christian R. Hayes https://orcid.org/0000-0003-2969-2445
Sten Hasselquist https://orcid.org/0000-0001-5388-0994
Keivan Stassun https://orcid.org/0000-0002-3481-9052
Marina Kounkel https://orcid.org/0000-0002-5365-1267
Don Dixon https://orcid.org/0000-0001-6977-9495
Guy S. Stringfellow https://orcid.org/0000-0003-1479-3059
Joleen K. Carlberg https://orcid.org/0000-0001-5926-4471
Borja Anguiano https://orcid.org/0000-0001-5261-4336
Nathan De Lee https://orcid.org/0000-0002-3657-0705
Nicholas W. Troup https://orcid.org/0000-0003-3248-3097

References

Ahumada, R., Prieto, C. A., Almeida, A., et al. 2020, ApJS, 249, 3
Badenes, C., & Maoz, D. 2012, ApJL, 749, L11
Badenes, C., Mazzola, C., Thompson, T. A., et al. 2018, ApJ, 854, 147
Bentley, J. L. 1975, Commun. ACM, 18, 509
Binney, J., & Tremaine, S. 2008, Galactic Dynamics (2nd ed.; Princeton, NJ: Princeton Univ. Press)
Blanton, M. R., Bershady, M. A., Abolfathi, B., et al. 2017, AJ, 154, 28
Buttry, R., Pace, A. B., Koposov, S. E., et al. 2022, MNRAS, 514, 1706
Fielder, C. E., Newman, J. A., Andrews, B. H., et al. 2021, MNRAS, 508, 4459
García Pérez, A. E., Allende Prieto, C., Holtzman, J. A., et al. 2016, AJ, 151, 144
Gibbons, S. L. J., Belokurov, V., & Evans, N. W. 2017, MNRAS, 464, 794
Gunn, J. E., Siegmund, W. A., Mannery, E. J., et al. 2006, AJ, 131, 2332
Hasselquist, S., Shetrone, M., Smith, V., et al. 2017, ApJ, 845, 162
Hayes, C. R., Majewski, S. R., Hasselquist, S., et al. 2020, ApJ, 889, 63
Gaia Collaboration, Helmi, A., van Leeuwen, F., et al. 2018, A&A, 616, A12

Holtzman, J. A., Shetrone, M., Johnson, J. A., et al. 2015, AJ, 150, 148
Hunter, J. D. 2007, CSE, 9, 90
Ibata, R. A., Gilmore, G., & Irwin, M. J. 1994, Natur, 370, 194
Jönsson, H., Holtzman, J. A., Prieto, C. A., et al. 2020, AJ, 160, 120
Koposov, S. E., Gilmore, G., Walker, M. G., et al. 2011, ApJ, 736, 146
Kramida, A., Ralchenko, Y. & NIST ASD Team 2021, NIST Atomic Spectra Database (ver. 5.9) (Gaithersburg, MD: National Institute of Standards and Technology) https://physics.nist.gov/asd
Licquia, T. C., Newman, J. A., & Brinchmann, J. 2015, ApJ, 809, 96
Majewski, S. R., Schiavon, R. P., Frinchaboy, P. M., et al. 2017, AJ, 154, 94
Maoz, D., Badenes, C., & Bickerton, S. J. 2012, ApJ, 751, 143
Marks, M., & Kroupa, P. 2011, MNRAS, 417, 1702
Martinez, G. D., Minor, Q. E., Bullock, J., et al. 2011, ApJ, 738, 55
Mazzola, C., Badenes, C., Moe, M., et al. 2020, MNRAS, 499, 499
McConnachie, A. W., & Côté, P. 2010, ApJL, 722, L209
McKinney, W. 2010, in Proc. 9th Python in Science Conference, ed. S. van der Walt & J. Millman, 56, https://conference.scipy.org/proceedings/scipy2010/mckinney.html
Minor, Q. E., Pace, A. B., Marshall, J. L., & Strigari, L. E. 2019, MNRAS, 487, 2961
Moe, M., & Di Stefano, R. 2017, ApJS, 230, 15
Moe, M., Kratter, K. M., & Badenes, C. 2019, ApJ, 875, 61
Nidever, D. L., Holtzman, J. A., Prieto, C. A., et al. 2015, AJ, 150, 173
Pedregosa, F., Varoquaux, G., Gramfort, A., et al. 2011, J. Mach. Learn. Res., 12, 2825
Perez, F., & Granger, B. E. 2007, CSE, 9, 21
Price-Whelan, A. M., Hogg, D. W., Foreman-Mackey, D., & Rix, H.-W. 2017, ApJ, 837, 20
Price-Whelan, A. M., Hogg, D. W., Rix, H.-W., et al. 2020, ApJ, 895, 2
Sanders, J. L., Belokurov, V., & Man, K. T. F. 2021, MNRAS, 506, 4321
Sanders, J. L., & Das, P. 2018, MNRAS, 481, 4093
Sbordone, L., Bonifacio, P., Buonanno, R., et al. 2007, A&A, 465, 815
Simon, J. D., Geha, M., Minor, Q. E., et al. 2011, ApJ, 733, 46
van der Walt, S., Colbert, S. C., & Varoquaux, G. 2011, CSE, 13, 22
Virtanen, P., Gommers, R., Oliphant, T. E., et al. 2020, NatMe, 17, 261
Wilson, J. C., Hearty, F. R., Skrutskie, M. F., et al. 2019, PASP, 131, 055001
Wyse, R. F. G., Moe, M., & Kratter, K. M. 2020, MNRAS, 493, 6109